

Busulfan in Infant to Adult Hematopoietic Cell Transplant Recipients: A Population Pharmacokinetic Model for Initial and Bayesian Dose Personalization

Jeannine S. McCune^{1,3}, Meagan J. Bemer¹, Jeffrey S. Barrett⁵, K. Scott Baker^{2,3,4}, Alan S. Gamis⁶, and Nicholas H.G. Holford⁷

Abstract

Purpose: Personalizing intravenous busulfan doses to a target plasma concentration at steady state (C_{ss}) is an essential component of hematopoietic cell transplantation (HCT). We sought to develop a population pharmacokinetic model to predict i.v. busulfan doses over a wide age spectrum (0.1–66 years) that accounts for differences in age and body size.

Experimental Design: A population pharmacokinetic model based on normal fat mass and maturation based on postmenstrual age was built from 12,380 busulfan concentration time points obtained after i.v. busulfan administration in 1,610 HCT recipients. Subsequently, simulation results of the initial dose necessary to achieve a target C_{ss} with this model were compared with pediatric-only models.

Results: A two-compartment model with first-order elimination best fit the data. The population busulfan clearance was 12.4 L/h for an adult male with 62 kg normal fat mass (equivalent to 70 kg total body weight). Busulfan clearance, scaled to body size—specifically normal fat mass, is predicted to be 95% of the adult clearance at 2.5 years postnatal age. With a target C_{ss} of 770 ng/mL, a higher proportion of initial doses achieved the therapeutic window with this age- and size-dependent model (72%) compared with dosing recommended by the U.S. Food and Drug Administration (57%) or the European Medicines Agency (70%).

Conclusion: This is the first population pharmacokinetic model developed to predict initial i.v. busulfan doses and personalize to a target C_{ss} over a wide age spectrum, ranging from infants to adults. *Clin Cancer Res*; 20(3); 754–63. ©2013 AACR.

Introduction

Allogeneic hematopoietic cell transplant (HCT) has curative potential for patients with either malignant or nonmalignant diseases (1). Busulfan is the most common chemotherapy agent used in HCT conditioning regimens that do not include total body irradiation. Considerable interpatient variability exists in the effectiveness and toxicity of busulfan-containing conditioning regimens when dosed on the basis of either body weight (mg/kg) or body surface area (BSA,

mg/m²; ref. 2). The variability in clinical outcomes is due, in part, to between-patient differences in busulfan pharmacokinetics and the narrow therapeutic window of busulfan systemic exposure (2). Rejection, relapse, and toxicity in HCT recipients are associated with busulfan plasma exposure, measured as area under the plasma–concentration time curve (AUC) or average steady-state concentration (C_{ss} ; calculated as $C_{ss} = \text{AUC}/\text{dosing frequency}$; ref. 2). Personalizing busulfan doses to a target plasma C_{ss} improves each of these clinical outcomes (as previously reviewed in ref. 2) and is clinically accepted in the context of the often-used intravenous administration route (3, 4). Because clinical practice is moving from every 6 hours (Q6h) to daily (Q24h) dosing frequency (2, 5, 6), the target exposure expressed using C_{ss} is preferable to AUC because C_{ss} (i.e., $C_{ss} = \text{AUC}/\text{dosing frequency}$) incorporates the dosing frequency.

More efficient methods of personalizing i.v. busulfan therapy are desirable for numerous reasons. First, relapse and nonrelapse mortality continue to be problematic even in the context of therapeutic drug monitoring (TDM) of i.v. busulfan (4, 5, 7). Second, the time delay to deliver a personalized busulfan dose recommendation with TDM presents a growing challenge with the increasing use of shorter i.v. busulfan courses, often administered as part of

Authors' Affiliations: University of Washington Schools of ¹Pharmacy and ²Medicine; ³Fred Hutchinson Cancer Research Center; ⁴Seattle Children's Hospital, Seattle, Washington; ⁵Division of Clinical Pharmacology & Therapeutics, The Children's Hospital of Philadelphia, Philadelphia, Pennsylvania; ⁶Children's Mercy Hospitals and Clinics, Kansas City, Missouri; and ⁷Department of Pharmacology and Clinical Pharmacology, University of Auckland, Auckland, New Zealand

Note: Supplementary data for this article are available at Clinical Cancer Research Online (<http://clincancerres.aacrjournals.org/>).

Corresponding Author: Jeannine S. McCune, Department of Pharmacy, University of Washington, Box 357630, Seattle, WA 98195. Phone: 206-543-1412; Fax: 206-543-3835; E-mail: jmccune@u.washington.edu

doi: 10.1158/1078-0432.CCR-13-1960

©2013 American Association for Cancer Research.

Translational Relevance

The alkylating agent busulfan is an integral part of many hematopoietic cell transplant conditioning regimens. Busulfan has a narrow therapeutic index, with data showing that busulfan plasma exposure is a predictive biomarker that forecasts response and toxicity. Intravenous busulfan doses are often personalized to a patient-specific exposure. Using the largest cohort of patients to date, this is the first i.v. busulfan population pharmacokinetic model that can predict initial i.v. busulfan doses and personalize exposure in infants through adults. This model accounts for differences in age and body size by use of normal fat mass. This age- and size-dependent model accurately estimates initial i.v. busulfan doses, which could allow for more rapidly obtaining the target exposure. Subsequent doses can be personalized by blending an individual patient's busulfan concentration–time data with this model to more accurately predict the dose required to achieve the target busulfan exposure.

reduced-intensity conditioning before HCT (1, 6) or gene therapy (8). An established method to improve TDM of i.v. busulfan is population pharmacokinetic modeling, which can characterize patient factors (covariates) such as weight and age that can be used to predict the initial (i.e., before TDM results are available) dose. Between-subject variability (BSV) and between-occasion variability (BOV, i.e., between dose) of a drug's pharmacokinetic disposition can be defined and these are useful for Bayesian dose adjustment (9–12). Population pharmacokinetic-based approaches have already been applied to TDM with oral busulfan (9) and i.v. cyclophosphamide (13) in HCT recipients. There is a clear need for improved initial i.v. busulfan dosing because current initial dosing practices have substantive variability and achieve the patient-specific therapeutic window of busulfan exposure in only 24.3% of children (3). Although various groups have created population pharmacokinetic models in children (Supplementary Table S1), most of the studies have been small, which makes identification of covariates problematic (14). Studies have typically focused on either pediatric or adult populations, requiring separate models for children and adults and limiting the generalizability of these models across the age continuum (10, 12). Our long-range goal is to improve outcomes in HCT recipients through more precise initial i.v. busulfan dosing and more effective TDM by more efficiently achieving the desired therapeutic window of busulfan exposure. Using the largest population of HCT recipients to date, we developed a population pharmacokinetic model over a wide age range to define busulfan pharmacokinetics regardless of age or body size with dosing guidance applicable from infants to adults. Subsequently, we compared initial i.v. busulfan dosing predictions with the age- and size-dependent model to predictions from recent i.v. busulfan

population pharmacokinetic models developed from pediatric populations (15–17).

Materials and Methods

Study population

Between June 1999 and September 2011, 1,610 HCT recipients aged 0.1 to 66 years underwent pharmacokinetic blood sampling to personalize i.v. busulfan doses (Table 1 and Supplementary Table S2) at the Fred Hutchinson Cancer Research Center (FHCRC) Pharmacokinetics Laboratory (1999–2001) or the Seattle Cancer Care Alliance (SCCA) Busulfan Pharmacokinetics Laboratory (2002–present). Approval of the FHCRC Institutional Review Board and Children's Oncology Group (COG, because AAML03P1 and AAML0531 participants were included) was obtained before analysis of anonymized data.

For clinical TDM purposes, demographic data (i.e., age, sex, height, weight) and clinical data (i.e., disease, which was subsequently categorized as malignant or not malignant as described in Supplementary Table S2) were requested from the treating institutions (Supplementary Table S3). For the 133 patients (108 adults and 25 children) treated under the auspices of a FHCRC protocol at a Seattle-based institution, the actual body weight (ABW), dosing weight (calculated as previously described; ref. 18), and ideal body weight (IBW) were available (i.e., "ABW-available cohort"). Institutions outside Seattle reliably provided only the busulfan dosing weight (DWT), which was calculated using their own institutional practices.

The initial busulfan dose, the dosing frequency, when the pharmacokinetic blood samples were obtained, and the acceptable therapeutic window of busulfan C_{ss} were chosen by the treating physician. Busulfan concentrations were determined by gas chromatography with mass spectrometry detection as previously described (3). The laboratory participated in routine cross-validation exercises between laboratories. The assay dynamic range was from 25 to 4,500 ng/mL, and the interday coefficient of variation was less than 8%. Ninety-one of 12,380 (0.7%) concentration time points were lower than the lower limit of quantitation (62 ng/mL); these measurements were included in the data set.

Population pharmacokinetic analysis

Busulfan administration was assumed to be zero-order, with the infusion duration described by the treating institution. Both 1- and 2-compartment models were examined. A 2-compartment model best fit the data with the lowest objective function value (OFV) and was used for all subsequent model construction.

Group parameter model

To characterize busulfan pharmacokinetics over the entire age continuum, all clearance (CL , Q) and volume (V_1 , V_2) parameters were scaled for body size and composition using allometric theory and predicted fat-free mass (FFM; refs. 19–21). The ABW-available cohort ($n = 133$) was used to estimate the fraction of fat mass (F_{fat}) contributing normal fat mass (NFM) for busulfan. F_{fat} is a drug- and

Table 1. Description of patient population

	ABW-available only	Overall
Number of patients	133	1610
Age, y	42.9 ± 20.7 (0.4–65.8)	9.8 ± 13.0 (0.1 to 65.8)
No. ≤ 4 y	16 (12%)	701 (43%)
Dosing weight (DWT, kg)	58.9 ± 22.3	30.2 ± 24.1
No. DWT ≤ 12 kg ^a	13 (10%)	466 (29%) ^a
Sex		
Male	72 (54%)	904 (56%)
Female	61 (46%)	689 (43%)
Not reported	0	17 (1%)
Diagnosis ^b		
Malignant	100 (75%)	978 (61%)
Not malignant	33 (25%)	632 (39%)
Dosing frequency ^c		
Q6h	39 (29%)	1387 (88%)
Q8h	0	9 (1%)
Q12h	0	8 (1%)
Q24h (daily)	94 (71%)	166 (11%)
No. of C _{ss} per patient ^d		
1	13 (10%)	1401 (87%)
2	3 (2%)	89 (6%)
3	117 (88%)	120 (7%)

NOTE: Data presented as number (%) or mean ± SD, percentages may not total 100 because of rounding.

^aPer FDA-approved package labeling.

^bSupplementary Table S2 details disease classifications.

^cUnknown for 40 patients who only had TDM after a test dose; percentages calculated from the remaining 1,570 patients.

^dC_{ss} used to express busulfan exposure because of the different dosing frequencies.

pharmacokinetic parameter-specific quantity; the value of F_{fat} was estimated for each pharmacokinetic parameter (21). Because ABW was not available for the remaining patients, these F_{fat} parameters were fixed in a second step when the overall cohort was used with an estimated value for total body weight (TBW) based on DWT (Supplementary Fig. S1; refs. 22, 23). FFM was predicted using equation (A):

$$FFM = WHS_{max} \times HT^2 \left(\frac{TBW}{WHS_{50} \times HT^2 + TBW} \right) \quad (A)$$

where WHS_{max} is the maximum FFM for any given height (HT, m) and WHS_{50} is the TBW value when FFM is half of WHS_{max} . WHS_{max} is 42.92 and 37.99 kg/m² and WHS_{50} is 30.93 and 35.98 kg/m² for males and females, respectively (19). The NFM was predicted using equation (B):

$$NFM = FFM + F_{fat} \times (TBW - FFM) \quad (B)$$

ABW was used for total body weight (TBW) when it was available, but for patients whose ABW was not available, TBW was predicted using equation (C):

$$TBW = DWT \times FDW \times FFEM_{DW} \quad (C)$$

where DWT is dosing weight provided by the treating institution, FDW is the fraction of DWT contributing to

TBW, and $FFEM_{DW}$ is the fraction of DWT that predicts the difference in TBW in women compared with men.

Size differences were described using equation (D). Following theory-based allometry (24), the allometric (P_{wr}) exponent in equation (D) was fixed to ³/₄ for CL and Q and 1 for V₁ and V₂.

$$F_{size} = \left(\frac{NFM}{70} \right)^{P_{wr}} \quad (D)$$

F_{size} is the fractional difference in allometrically scaled size compared with a 70 kg NFM individual. The NFM of 62 kg for CL and 59 kg for V correspond to an allometrically scaled TBW of 70 kg. A sigmoid E_{max} model was used to describe the maturation of busulfan CL based on postmenstrual age (PMA) using equation (E):

$$F_{mat} = \left(\frac{1}{1 + \left(\frac{PMA}{TM_{50}} \right)^{-Hill}} \right) \quad (E)$$

where F_{mat} is the fraction of the adult busulfan clearance value, TM_{50} is the PMA at which maturation is 50% of the adult value, and Hill defines the steepness of the change with PMA (20, 21). PMA was estimated by adding a gestational age of 40 weeks to postnatal age (PNA; ref. 25).

Differences associated with binary covariates [e.g., sex (F_{sex}) and disease (F_{disease})] were described on the basis of the fractional difference of pharmacokinetic parameter between the 2 groups. Once all the covariates were defined, covariate factors were combined to predict busulfan clearance for that specific group (CL_{GRP}). Group clearance includes those covariates identified in the model to characterize that specific population's pharmacokinetic parameters (equation F):

$$CL_{\text{GRP}} = CL_{\text{pop}} \times F_{\text{mat}} \times F_{\text{size}} \times F_{\text{sex}} \quad (\text{F})$$

where CL_{pop} is the overall population value of parameter. A similar model was used for intercompartmental clearance (Q), with F_{mat} and F_{sex} fixed to 1, and for V_1 and V_2 , with F_{mat} fixed to 1.

Random effects

Individual parameter model. Population parameter variability (PPV) was described using an exponential model for the random effects (equation G):

$$P_{ij} = P_{\text{pop}} \times \exp(\eta_i + \kappa_j) \quad (\text{G})$$

where P_{ij} is the parameter value for the i th individual on the j th occasion, and P_{pop} is the population value for the population parameter P (e.g., CL). The random effect model for BSV on TBW was proportional to TBW (equation H):

$$TBW_{ij} = TBW_{\text{pop}} \times (1 + \eta_i) \quad (\text{H})$$

Only BSV was estimated for TBW under the assumption that the same DWT method was used on all occasions for an individual patient.

Observation model. Residual unidentified variability (RUV) was described by assuming a combined model with proportional and additive normal distributions of random differences of the observed concentration-time data from the predicted concentration-time data. BSV in the residual error model was estimated for each observation by obtaining estimates of proportional ($\theta_{\text{RUV}_{\text{CV}}}$) and additive ($\theta_{\text{RUV}_{\text{SD}}}$) residual error parameters. The BSV of the RUV random effect ($\eta_{\text{PPV}_{\text{RUV}_i}}$) was estimated (22). The ε random effect was fixed with a unit variance (equation J):

$$SD_{ij} = \text{sqrt}((C_{ij} \times \theta_{\text{RUV}_{\text{CV}}})^2 + \theta_{\text{RUV}_{\text{SD}}}^2) \times e^{\eta_{\text{PPV}_{\text{RUV}_i}}} \quad (\text{I})$$

$$Y = C_{ij} + SD_{ij} \times \varepsilon \quad (\text{J})$$

where C_{ij} is the predicted concentration in the i th individual at the j th measurement time.

Model selection and evaluation

Model selection was based on bootstrap parameter confidence intervals, OFV, and the plausibility of visual predictive check (VPC) plots. Measures of parameter imprecision were computed using bootstrap methods (26, 27). VPCs were used to evaluate the overall predictive performance of the model for concentrations (28). Prediction-corrected VPCs were used to account for differences in covariates and dose adjustments based on previous concentrations (29).

Initial dosing prediction

The initial busulfan dose for Q6h dosing frequency is provided by both the U.S. Food and Drug Administration (FDA) and the European Medicines Agency (EMA) product labels, as described in Supplementary Table S1. The FDA dosing is based upon the modeling of Booth and colleagues (30), which recommends busulfan dosing based on ABW in children. In adults, the FDA model recommends using either ABW or ideal body weight, or adjusted ideal body weight (AIBW; equation K) for obese patients.

$$AIBW = IBW + 0.25 \times (TBW - IBW) \quad (\text{K})$$

This differs from the EMA dosing, which is based upon the modeling of Nguyen and colleagues (31), and has 5 dosing increments based on either ABW (for children who are not obese) or AIBW in obese adults. We evaluated the EMA dosing, using TBW for obese children and AIBW for obese adults. A body mass index greater than 28 kg/m² was used to define obesity, and IBW or AIBW was applied only for age > 16 years (adult) because the IBW calculation may give negative values in children. Using the EMA dosing, we also evaluated the clearance prediction models from 3 recently published studies (15–17) to calculate initial dose.

After final model construction, dosing simulations were conducted to estimate the initial i.v. busulfan dose using a daily (i.e., Q24h) dosing frequency. Linear pharmacokinetics after Q6h and Q24h dosing frequency have been reported with i.v. busulfan (32). Thus, the initial dosing can be adjusted for any dosing frequency (e.g., dividing by 4 to obtain the initial dose with Q6h dosing frequency). Busulfan target exposure is expressed as C_{ss} , which is preferable to AUC because C_{ss} incorporates dosing frequency (i.e., $C_{\text{ss}} = \text{AUC}/\text{dosing frequency}$). The FDA and EMA dosing simulation had a busulfan target AUC of 1,125 $\mu\text{mol}/\text{L} \times \text{min}$ with a Q6h dosing frequency (30, 31), which equates to a C_{ss} of 770 ng/mL. Therefore, a target C_{ss} of 770 ng/mL was used for dosing simulations. To determine those within an acceptable range, the therapeutic window for bioequivalence—widely used for drugs with a narrow therapeutic index—was used. It was set as no greater than 25% higher and no less than 20% lower than the target. Therefore, the acceptable therapeutic window equals 592 to 963 ng/mL.

Computation

Nonlinear models were developed using NONMEM (Version 7 Level 2.0; ref. 33) and Wings for NONMEM (34). The first-order conditional estimate method with the interaction option was used with PREDPP library models. A convergence criterion of 3 significant digits was used to identify successful minimization. Computation was conducted using Intel Xeon, Pentium, Core, or Athlon MP2000 processors with Microsoft Windows 2003, Windows XP, or Windows 7. The Intel Visual Fortran compiler (Version 11) with compiler options of /nologo/nbs/w/4Yportlib/Gs/Ob1gyti/Qprec_div was used to compile NONMEM.

Results

Patient characteristics

Patient pretransplant demographics and HCT characteristics are described in Table 1 with a more detailed description in Supplementary Table S2. For the overall patient population, the mean age was 9.8 years (range, 0.1–65.8); the majority (92%) were younger than 20 years. The majority (904 of 1,610, 56%) of the patients were male. The gestational age and PNA were not available; the gestational age was calculated assuming that all infants were of 40 weeks gestation. Of the 466 infants (<2 years old), 256 were less than 1 year and 25 were less than 3 months PNA. There were 701 patients (44%) less than 4 years old, which is the dosing threshold for COG studies, and 451 patients (28%) weighed less than 12 kg, at which weight higher initial i.v. busulfan doses are recommended per the FDA package insert (30).

Structural model

The final model consisted of 2 compartments for distribution with first-order elimination. There was no evidence for mixed order elimination. Bootstrap population parameter estimates from the age- and size-dependent model using theory-based allometry are summarized in Table 2. The shrinkage of the random effects for the structural parameters was CL = 17%, V_1 = 31%, Q = 31%, and V_2 = 38%. Regarding the distribution process, a sample drawn exactly at the end of the infusion may be too soon to reflect the distribution process predicted from the model. A subset of the data excluding concentration time points drawn within 5 minutes of the end of the infusion was used with the model developed from all of the data. The parameter estimates were very similar, suggesting that there was no important bias introduced from including the end of infusion concentration time points.

Table 2. Population pharmacokinetic parameters estimates with theory-based allometric exponents (100 bootstrap replications)

Parameter	Description	Units ^a	Bootstrap estimate (RSE%)
CL	Clearance	L/h/62 kg NFM CL	11.4 (1.1)
V_1	Central volume of distribution	L/59 kg NFM V	13.9 (6.6)
Q	Inter-compartmental clearance	L/h/62 kg NFM CL	135.2 (7.2)
V_2	Peripheral volume of distribution	L/59 kg NFM V	29.9 (3.0)
$F_{Fat_CL}^b$	Fat fraction for clearance	—	0.509 (42.8)
$F_{Fat_V}^b$	Fat fraction for volume	—	0.203 (51.6)
TM50 _{CL}	PMA at 50% maturation	—	45.7 (4.3)
HILL _{CL}	Hill coefficient for maturation	—	2.3 (9.7)
F_{FEM_V}	Fractional difference in total volume ($V_1 + V_2$) in females	—	1.07 (1.2)
F_{FEM_DW}	Fractional difference in dosing weight in females	—	1.08 (1.7)
F_{T1_CL}	Fraction of 0–6 h clearance >6 and <36 h	—	0.932 (1.2)
F_{T2_CL}	Fraction of 0–6 h clearance \geq 36 h	—	0.919 (1.4)
Between-subject variability (BSV) ^a			
TBW			0.166 (7.8)
CL			0.215 (4.7)
V_1			0.410 (10.8)
Q			0.922 (9.1)
V_2			0.120 (23.8)
Between-occasion variability (BOV) ^b			
CL			0.113 (14.8)
V_1			0.244 (20.0)
Q			0.577 (24.6)
V_2			0.212 (12.4)
RUV _{ADD} ^c	Additive residual unidentified variability	ng/mL	26.2 (13.7)
RUV _{PROP} ^c	Proportional residual unidentified variability	.	0.0387 (12.8)

^aThe NFM of 62 kg for CL and 59 kg for V correspond to allometrically scaled total body weight of 70 kg.

^bBootstrap estimates for F_{FAT_CL} and F_{FAT_V} from ABW available data only.

^cRandom effects are expressed as the square root of the estimated variance. BSV and BOV estimates are the apparent coefficient of variation of the variability.

Group parameter model

Because of the large number of patients and the wide-spread body sizes, we estimated the allometric exponents for each of the 4 main pharmacokinetic parameters (Supplementary Table S4). Initial estimates of $2/3$ and 1.25 were used for the clearance and volume exponents. Theory-based exponents were confirmed for CL ($3/4$), V_1 and V_2 (1) (Table 2). The confidence interval for the intercompartmental clearance between V_1 and V_2 (Q) included the theory-based values for both clearances and volumes, so no conclusion could be drawn about the use of a theory-based value of $3/4$. When ABW was not available, it was estimated from DWT and sex (equation C). The fraction of dosing weight (FDW) that predicted TBW was indistinguishable from 1 and was fixed to 1 but predicted TBW was 8% higher in women (F_{FEM_DW}). The predicted distribution of TBW was similar to that of ABW in children with DWT <40 kg; however, the TBW was higher than DWT in adults as expected if DWT is based on AIBW (Supplementary Fig. S1). The estimates of the size-dependent parameters are expressed per 62 kg of NFM in an adult. On the basis of the ABW-available data set, the F_{fat} for clearance is 0.509 and for the volume of the central compartment (V_1) is 0.203. These values indicate that the biologically effective body size determining clearance is proportional to FFM plus 51% of fat mass, whereas for volume it is proportional to FFM plus 20% of fat mass. As shown by the VPC (Fig. 1, Supplementary Fig. S2), this age and size model accurately described busulfan pharmacokinetics over the entire age continuum (0.1–65.8 years). The maturation of busulfan clearance reaches 50% of adult values at 46 weeks PMA, that is, 6 weeks after birth assuming a full-term gestational age of 40 weeks. Size-standardized clearance reaches 95% of adult values at 2.5 postnatal years (Fig. 2). In addition, busulfan clearance decreases over time. Compared with the clearance from 0 to 6 hours, the clearance from 6 to 36 hours was 6.8% lower and from 36 to 83 hours was 8.1% lower.

Female sex was associated with a 7% higher volume of distribution (central and peripheral volume; 11.9 units smaller OFV in ABW-available data set and 35.4 units smaller with the full data set) but there was no effect of sex on clearance. There was no difference in clearance or volume of distribution in patients who had malignancy as their primary diagnosis ($n = 978$) compared with patients with nonmalignant diseases ($n = 632$).

Random-effects model

Both BSV and BOV were included to account for the potential influence of various factors on busulfan pharmacokinetics, including sex and disease (malignant vs. non-malignant; Supplementary Table S5). The BSV was moderate for clearance, with greater BSV for the volumes of distribution (V_1 and V_2) and the intercompartmental clearance between V_1 and V_2 (Q). A similar trend was observed for the BOV. The BSV and BOV for clearance had apparent coefficients of variation of 21.5% and 11.3%, respectively. The BSV around TBW had an apparent coefficient of variation of 16.0%.

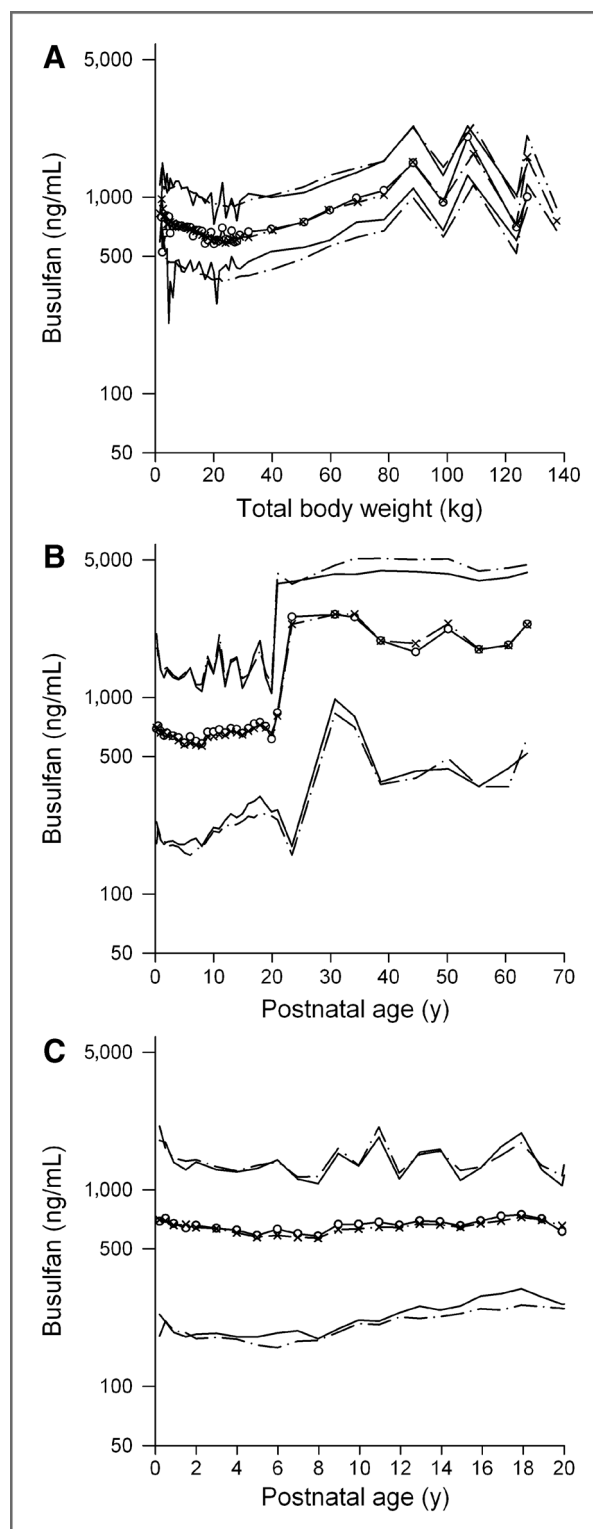


Figure 1. VPCs by total body weight for overall cohort (A), by PNA for the overall cohort (B), and by PNA for children (C). Dashed lines represent the 5th and 95th percentiles of the observed data. Solid lines represent the 5th and 95th percentiles of simulated data. Open circles and crosses represent 50th percentile of observed and simulated data. Please note that most adults received daily i.v. busulfan as per the clinical protocol at the time.

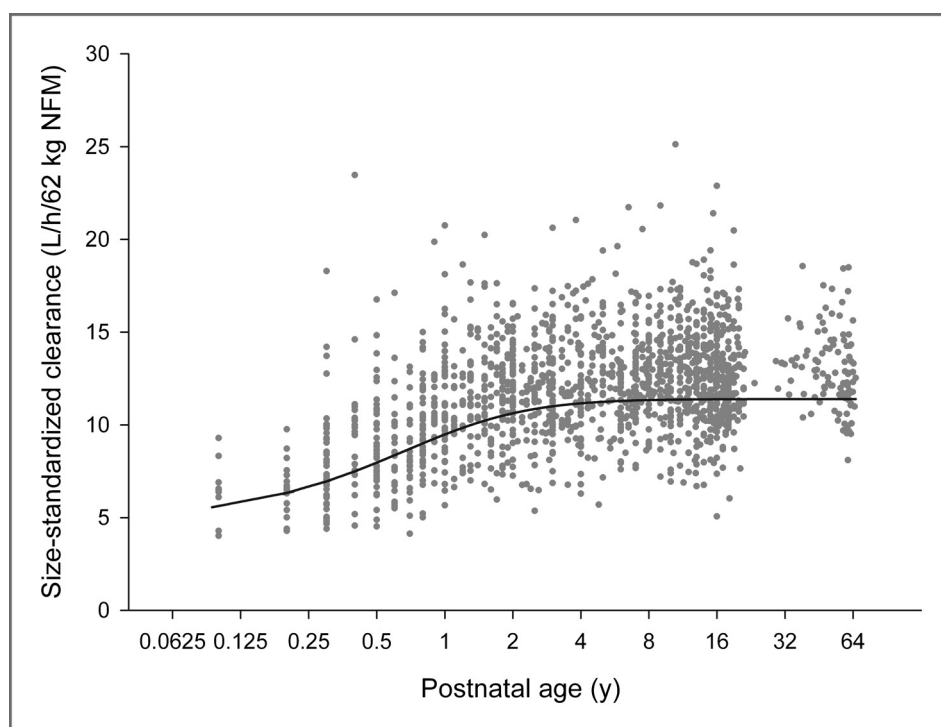


Figure 2. Maturation of size-standardized i.v. busulfan clearance, as L/h/62 kg NFM. Symbols are empirical Bayes estimates scaled to 62 kg NFM. The solid line is the predicted maturation function for i.v. busulfan clearance.

Comparison with recent i.v. busulfan population pharmacokinetic models

By creating this model using data from such a wide age range, we sought to define busulfan pharmacokinetics regardless of age or body size to guide i.v. busulfan dosing and TDM for any patient with just one model. Our age- and size-dependent model accounted for physiologically based differences in body composition and ontology over the age range. To evaluate the prediction accuracy in children, we examined recently published busulfan pharmacokinetic models created from pediatric datasets (15–17). These models were tested by re-estimating the model parameters using our data set (Supplementary Table S6). The Paci and Bartelink models used empirical allometric models for clearance to account for size and maturation, whereas the Trame model used theory-based allometry without accounting for maturation (Supplementary Table S1). The current data set was more accurately described with the age- and size-dependent model using NFM. Specifically, the Paci model had a worse OFV by 1,594 units with the ABW-available data set and by 6,446 units when the full data set was used. The Bartelink model had a worse OFV by 911 units with the ABW-available data set and by 4,097 units when the full data set was used. Similarly, the Trame model had a worse OFV by 1,025 units with ABW-available data set and by 5,488 units when the full data set was used.

Comparison of initial dosing predictions

The empirical Bayes estimate of clearance from our age- and size-dependent model was used to calculate the daily dose of busulfan to maintain the target C_{ss} of 770 ng/mL.

These individual estimates are expected to be quite precise because the Bayesian shrinkage was only 17%. The initial i.v. busulfan dose predictions using our age- and size-dependent model (detailed in Materials and Methods and Supplementary Table S7) were compared with the FDA and EMA dosing (Table 3). Our age- and size-dependent model led to a higher percentage of patients achieving the therapeutic window compared with the FDA dosing in the entire population ($P < 0.0001$), with the differences lying in children younger than 10 years. A similar percentage of patients would achieve the therapeutic window using the EMA dosing compared with our age- and size-dependent model in the entire population ($P = 0.214$), with a statistically—but most likely not clinically—significant difference in children between 10 and <15 years. Our age- and size-dependent model had comparable performance to the recent i.v. busulfan population pharmacokinetic models (Supplementary Table S6).

Discussion

We sought to create an i.v. busulfan pharmacokinetic model that is generalizable to all patients, which was achieved by using this age- and size-dependent model (Table 2). Our main findings are: (i) this age- and size-dependent model accurately predicts i.v. busulfan concentrations over a wide range of body weights and ages (Fig. 1); (ii) i.v. busulfan clearance, scaled to size (i.e., NFM), reaches 95% of adult values at 2.5 postnatal years (Fig. 2); (iii) the model yields similar pharmacokinetic parameters compared with recently reported population pharmacokinetic models from smaller, exclusively pediatric populations; (iv) initial dosing predictions indicate that our age- and size-

Table 3. Comparison of accuracy of model-based i.v. busulfan dose predictions by model and age group to achieve the therapeutic window for busulfan C_{ss} of 592 to 963 ng/mL

Age, y	% in therapeutic window by method (P^a)		
	Age- and size-dependent model	FDA ^b	EMA
All ($n = 1610^c$)	72%	57% (<.0001)	70% (0.214)
≥ 20 ($n = 128$)	82%	83% (0.87)	84% (0.616)
15 to <20 ($n = 224$)	76%	78% (0.575)	80% (0.305)
10 to <15 ($n = 238$)	77%	68% (0.031)	65% (0.005)
5 to <10 ($n = 249$)	78%	49% (<.0001)	71% (0.081)
2 to <5 ($n = 304$)	70%	33% (<.0001)	71% (0.79)
1 to <2 ($n = 210$)	69%	54% (0.001)	72% (0.521)
< 1 ($n = 256$)	62%	54% (0.060)	61% (0.785)

^a P from χ^2 analysis of the number of patients within the therapeutic window by dosing method compared with the age- and size-dependent model.

^bThe product labeling doses for Q6h dosing frequency are as follows: FDA dosing is 1.1 mg/kg for ≤ 12 kg and 0.8 mg/kg for > 12 kg. EMA dosing is 1 mg/kg for < 9 kg, 1.2 mg/kg for 9 to < 16 kg, 1.1 mg/kg for 16 to 23 kg, 0.95 mg/kg for > 23 to 34 kg, and 0.8 mg/kg for > 34 kg. COG trials AAML03P1 and AAML0531 recommended initial busulfan doses for Q6h dosing frequency: 0.8 mg/kg for < 10 kg, 1 mg/kg for ≥ 10 kg and ≤ 4 years old, 0.8 mg/kg for > 4 years old.

^cAge was unavailable for one patient.

dependent model performs well compared with other methods, especially FDA dosing guidelines (Table 3).

This study has provided the first adequately powered test confirming theory-based allometry for clearance and volume parameters. The maturation of clearance in infants has been described for many drugs using a sigmoid function of PMA (21). Although the function is empirical, it has physiologic limits. Specifically, these limits predict a clearance of zero at conception and approach adult values as maturation is completed. We have applied the same maturation function to busulfan and find that maturation reaches 50% of adult values at 46 weeks PMA. Busulfan clearance reaches 95% of adult values at 2.5 postnatal years. An earlier analysis of a subset of the current data that found children less than 4 years of age had lower busulfan clearance than adults using BSA scaling without considering body composition (3). Using physiologically based descriptions of body composition and theory-based allometric principles, we have shown that busulfan clearance and volume are predicted neither by TBW nor by FFM, but by a size that lies between the 2. We recognize that our dataset is limited because ABW was available in only 133 patients. However, DWT was available for all 1,610 patients; many of the previously published busulfan population pharmacokinetic models were created with only DWT (Supplementary Table S1). There are few population pharmacokinetic models of i.v. busulfan from adults [$n = 37$ (12) to 127 (10)]. It should be appreciated that our age- and size-dependent model was constructed using data from one of the largest studies in adults ($n = 128$). Likewise, the age- and size-dependent model may also improve i.v. busulfan dosing in the obese. The paucity of pharmacokinetic data for chemotherapy dosing in obese patients is gaining attention, and

pooling data from previous studies to test chemotherapy dosing recommendations for obese patients has recently been encouraged (35). Validation of the model in adult populations—particularly the obese—is needed, as our results clearly show our age- and size-dependent model predicts busulfan pharmacokinetics as well as the existing models generated from pediatric data (Supplementary Table S6). Notably, busulfan pharmacokinetic parameters were not influenced by disease (malignant vs. nonmalignant), which is consistent with previous data (3, 36). Also consistent with previous data (37, 38) was our observation of a slight decrease in busulfan clearance over time.

This data set was obtained from 51 institutions that were targeting i.v. busulfan doses for clinical purposes, thus providing an accurate assessment of the challenges of personalizing doses based on pharmacokinetics (i.e., TDM). Only a minority of concentrations (367 of 12,747, see Supplementary Methods) were considered problematic, proving that TDM is feasible in a clinical setting. Our recent analysis of prescribing patterns in 729 pediatric HCT recipients revealed that the initial busulfan dose achieved the target exposure in only 24.3% of children (3). Appreciable debate about the optimal initial i.v. busulfan dose has resulted from the Trame report (15, 39). The FDA dosing guidance was based on simulations using a pediatric population pharmacokinetic model that indicated that about 60% of children would achieve a busulfan C_{ss} between 615 and 925 ng/mL (30). Nguyen and colleagues had developed a 5-category dosing guideline (i.e., EMA dosing) that was expected to achieve a mean busulfan C_{ss} of 770 ng/mL based on a different pediatric population pharmacokinetic model (31). The success of the EMA dosing guidance to achieve a busulfan C_{ss} of 615 to 1,025 ng/mL without TDM has been

variable (15, 40–42). Recently, Trame and colleagues created a busulfan population pharmacokinetic model from 94 children receiving oral ($n = 54$) or i.v. ($n = 40$) busulfan (15). Their simulations revealed that only 44% of children would achieve a busulfan C_{ss} of 615 to 1,025 ng/mL when EMA dosing was used without TDM and that a higher proportion (70%–71%) would achieve this therapeutic window with dosing based on BSA or allometric body weight. Our age- and size-dependent model conducted similarly to the Trame model (Supplementary Table 6). In addition, compared with FDA dosing, our model can more accurately estimate the initial i.v. busulfan dose to more rapidly achieve the therapeutic busulfan C_{ss} (Table 3). Our model did appreciably better than FDA dosing for children younger than 10 years and achieved a similar percentage within the therapeutic window as the EMA dosing. The generalizability of our model provides a robust tool for prescribers to dose busulfan with minimal concern about the original population from which the model was constructed.

To our knowledge, we are the first to describe the maturation of i.v. busulfan clearance; our data modeling indicates that at 2.5 years of age i.v. busulfan clearance is essentially (95th percentile) that of adults. Collection of PMA would be useful for implementation of this model for estimating i.v. busulfan clearance in children younger than 2.5 years. These covariates can be used for initial i.v. busulfan dosing and also for TDM. Dose prediction can be based on a prescriber-chosen target exposure. There has been a practice trend towards a Q24h instead of the traditional Q6h dosing frequency (2). A target exposure expressed using C_{ss} is preferable to expression using AUC because C_{ss} (i.e., $C_{ss} = \text{AUC}/\text{dosing frequency}$) incorporates the dosing frequency. This allows the prescriber to choose a single target C_{ss} and dosing frequency independently. Subsequent dose personalization can take place using measured busulfan concentrations. The estimated BOV in clearance (11.3%) indicates that 95% of patients can expect to achieve a C_{ss} within the 80% to 125% acceptable therapeutic window (43) with appropriate dose adjustment.

In conclusion, we built a novel population pharmacokinetic model, reliant on the largest busulfan database to date, that spans a wide age range (i.e., neonates to adults), accounting for age, body weight, and body composition (i.e., NFM). The model is based on principles that have

already been shown to be robust for predictions with other small molecule agents from neonates to adults (44). Future work should focus on incorporation of this model into a decision support system that includes relevant clinical data in a user-friendly interface to clearly communicate the optimal busulfan dose for HCT recipients. This model can accurately estimate the initial busulfan dose, hopefully improving upon the current initial dosing practices in which only 24.3% of children achieve the patient-specific therapeutic window of busulfan exposure (3). Furthermore, by including pharmacokinetic sampling, this model can also be used for more efficient TDM by using Bayesian predictions for personalized busulfan dosing, which has been previously used in HCT recipients (9, 13).

Disclosure of Potential Conflicts of Interest

J.S. McCune has received a commercial research grant from Otsuka Pharmaceutical of North America. No potential conflicts of interest were disclosed by the other authors.

Authors' Contributions

Conception and design: J.S. McCune, A.S. Gomis, N.H.G. Holford
Development of methodology: J.S. McCune, J.S. Barrett, N.H.G. Holford
Acquisition of data (provided animals, acquired and managed patients, provided facilities, etc.): J.S. McCune, A.S. Gomis
Analysis and interpretation of data (e.g., statistical analysis, biostatistics, computational analysis): J.S. McCune, M.J. Bemer, K.S. Baker, N.H.G. Holford
Writing, review, and/or revision of the manuscript: J.S. McCune, M.J. Bemer, J.S. Barrett, K.S. Baker, A.S. Gomis, N.H.G. Holford
Administrative, technical, or material support (i.e., reporting or organizing data, constructing databases): J.S. McCune, M.J. Bemer, J.S. Barrett
Study supervision: J.S. McCune, A.S. Gomis

Acknowledgments

The authors thank Erin Dombrowsky for her invaluable assistance in streamlining data integration through the development of SAS macros.

Grant Support

This work was supported by, in part, research funding from Otsuka Pharmaceutical of North America (J.S. McCune), UW DMTPR (J.S. McCune), University of Auckland (NHGH), Children's Oncology Group Chair's grant NIH U10 CA98543 (A.S. Gomis), SDC U10 CA98413 (A.S. Gomis), U10 HD037255 (J.S. Barrett), and RC1 LM010367-01 (J.S. Barrett).

The costs of publication of this article were defrayed in part by the payment of page charges. This article must therefore be hereby marked *advertisement* in accordance with 18 U.S.C. Section 1734 solely to indicate this fact.

Received July 17, 2013; revised October 25, 2013; accepted November 6, 2013; published OnlineFirst November 11, 2013.

References

- Deeg HJ, Maris MB, Scott BL, Warren EH. Optimization of allogeneic transplant conditioning: not the time for dogma. *Leukemia* 2006;20:1701–5.
- McCune JS, Holmberg LA. Busulfan in hematopoietic stem cell transplant setting. *Expert Opin Drug Metab Toxicol* 2009;5:957–69.
- McCune JS, Baker KS, Blough DK, Gomis A, Bemer MJ, Kelton-Rehkopf MC, et al. Variation in prescribing patterns and therapeutic drug monitoring of intravenous busulfan in pediatric hematopoietic cell transplant recipients. *J Clin Pharmacol* 2013;53:264–75.
- Nieto Y, Thall P, Valdez B, Andersson B, Popat U, Anderlini P, et al. High-dose infusional gemcitabine combined with busulfan and melphalan with autologous stem-cell transplantation in patients with refractory lymphoid malignancies. *Biol Blood Marrow Transplant* 2012;18:1677–86.
- Geddes M, Kangaroo SB, Naveed F, Quinlan D, Chaudhry MA, Stewart D, et al. High busulfan exposure is associated with worse outcomes in a daily i.v. busulfan and fludarabine allogeneic transplant regimen. *Biol Blood Marrow Transplant* 2008;14:220–8.
- Kletzel M, Jacobsohn D, Duerst R. Pharmacokinetics of a test dose of intravenous busulfan guide dose modifications to achieve an optimal area under the curve of a single daily dose of intravenous busulfan in children undergoing a reduced-intensity conditioning regimen with

- hematopoietic stem cell transplantation. *Biol Blood Marrow Transplant* 2006;12:472–9.
7. McCune JS, Woodahl EL, Furlong T, Storer B, Wang J, Heimfeld S, et al. A pilot pharmacologic biomarker study of busulfan and fludarabine in hematopoietic cell transplant recipients. *Cancer Chemother Pharmacol* 2012;69:263–72.
 8. Aiuti A, Slavin S, Aker M, Ficara F, Deola S, Mortellaro A, et al. Correction of ADA-SCID by stem cell gene therapy combined with nonmyeloablative conditioning. *Science* 2002;296:2410–3.
 9. Bleyzac N, Souillet G, Magron P, Janoly A, Martin P, Bertrand Y, et al. Improved clinical outcome of paediatric bone marrow recipients using a test dose and Bayesian pharmacokinetic individualization of busulfan dosage regimens. *Bone Marrow Transplant* 2001;28:743–51.
 10. Nguyen L, Leger F, Lennon S, Puozzo C. Intravenous busulfan in adults prior to haematopoietic stem cell transplantation: a population pharmacokinetic study. *Cancer Chemother Pharmacol* 2006;57:191–8.
 11. Bertholle-Bonnet V, Bleyzac N, Galambrun C, Mialou V, Bertrand Y, Souillet G, et al. Influence of underlying disease on busulfan disposition in paediatric bone marrow transplant recipients: a nonparametric population pharmacokinetic study. *Ther Drug Monit* 2007;29:177–84.
 12. Salinger DH, Vicini P, Blough DK, O'Donnell PV, Pawlikowski MA, McCune JS. Development of a population pharmacokinetics-based sampling schedule to target daily intravenous busulfan for outpatient clinic administration. *J Clin Pharmacol* 2010;50:1292–300.
 13. McCune JS, Batchelder A, Guthrie KA, Witherspoon R, Appelbaum FR, Phillips B, et al. Personalized dosing of cyclophosphamide in the total body irradiation-cyclophosphamide conditioning regimen: a phase II trial in patients with hematologic malignancy. *Clin Pharmacol Ther* 2009;85:615–22.
 14. Ribbing J, Jonsson EN. Power, selection bias and predictive performance of the Population Pharmacokinetic Covariate Model. *J Pharmacokinet Pharmacodyn* 2004;31:109–34.
 15. Trame MN, Bergstrand M, Karlsson MO, Boos J, Hempel G. Population pharmacokinetics of busulfan in children: increased evidence for body surface area and allometric body weight dosing of busulfan in children. *Clin Cancer Res* 2011;17:6867–77.
 16. Bartelink IH, Boelens JJ, Bredius RG, Egberts AC, Wang C, Bierings MB, et al. Body weight-dependent pharmacokinetics of busulfan in paediatric haematopoietic stem cell transplantation patients: towards individualized dosing. *Clin Pharmacokinet* 2012;51:331–45.
 17. Paci A, Vassal G, Moshous D, Dalle JH, Bleyzac N, Neven B, et al. Pharmacokinetic behavior and appraisal of intravenous busulfan dosing in infants and older children: the results of a population pharmacokinetic study from a large pediatric cohort undergoing hematopoietic stem-cell transplantation. *Ther Drug Monit* 2012;34:198–208.
 18. Gibbs JP, Gooley T, Comeau B, Murray G, Stewart P, Appelbaum FR, et al. The impact of obesity and disease on busulfan oral clearance in adults. *Blood* 1999;93:4436–40.
 19. Janmahasatian S, Duffull SB, Ash S, Ward LC, Byrne NM, Green B. Quantification of lean bodyweight. *Clin Pharmacokinet* 2005;44:1051–65.
 20. Anderson BJ, Holford NH. Mechanism-based concepts of size and maturity in pharmacokinetics. *Annu Rev Pharmacol Toxicol* 2008;48:303–32.
 21. Anderson BJ, Holford NH. Mechanistic basis of using body size and maturation to predict clearance in humans. *Drug Metab Pharmacokinet* 2009;24:25–36.
 22. Karlsson MO, Jonsson EN, Wiltse CG, Wade JR. Assumption testing in population pharmacokinetic models: illustrated with an analysis of moxonidine data from congestive heart failure patients. *J Pharmacokin Biopharm* 1998;26:207–46.
 23. Mould DR, Holford NH, Schellens JH, Beijnen JH, Hutson PR, Rosing H, et al. Population pharmacokinetic and adverse event analysis of topotecan in patients with solid tumors. *Clin Pharmacol Ther* 2002;71:334–48.
 24. West GB, Brown JH, Enquist BJ. The fourth dimension of life: fractal geometry and allometric scaling of organisms. *Science* 1999;284:1677–9.
 25. Engle WA American Academy of Pediatrics Committee on Fetus and Newborn. Age terminology during the perinatal period. *Pediatrics* 2004;114:1362–4.
 26. Parke J, Holford NH, Charles BG. A procedure for generating bootstrap samples for the validation of nonlinear mixed-effects population models. *Comput Methods Programs Biomed* 1999;59:19–29.
 27. Holford NHG, Kirkpatrick C, Duffull SB. NONMEM termination status is not an important indicator of the quality of bootstrap Parameter Estimates Population Approach Group in Europe (PAGE); 2006; Bruges. Available from: <http://www.page-meeting.org/default.asp?abstract=992>.
 28. Holford NHG. The Visual Predictive Check – Superiority to Standard Diagnostic (Rorschach) Plots. Abstracts of the Annual Meeting of the Population Approach Group in Europe (PAGE) 2005;14:Abstr 738.
 29. Bergstrand M, Hooker AC, Wallin JE, Karlsson MO. Prediction-corrected visual predictive checks for diagnosing nonlinear mixed-effects models. *AAPS J* 2011;13:143–51.
 30. Booth BP, Rahman A, Dagher R, Griebel D, Lennon S, Fuller D, et al. Population pharmacokinetic-based dosing of intravenous busulfan in pediatric patients. *J Clin Pharmacol* 2007;47:101–11.
 31. Nguyen L, Fuller D, Lennon S, Leger F, Puozzo C. I.V. busulfan in pediatrics: a novel dosing to improve safety/efficacy for hematopoietic progenitor cell transplantation recipients. *Bone Marrow Transplant* 2004;33:979–87.
 32. Madden T, de Lima M, Thapar N, Nguyen J, Roberson S, Couriel D, et al. Pharmacokinetics of once-daily IV busulfan as part of pretransplantation preparative regimens: a comparison with an every 6-hour dosing schedule. *Biol Blood Marrow Transplant* 2007;13:56–64.
 33. Beal SL, Sheiner LB, Boeckmann AJE. NONMEM users guides. Elliott City, MD: Icon Development Solutions; 1989–2006.
 34. Holford NHG. Wings for NONMEM Version 720 for NONMEM 7.2 2011. Available from: <http://wfn.sourceforge.net>. [Last accessed 25 Nov 2013].
 35. Griggs JJ, Mangu PB, Anderson H, Balaban EP, Dignam JJ, Hryniuk WM, et al. Appropriate chemotherapy dosing for obese adult patients with cancer: American Society of Clinical Oncology clinical practice guideline. *J Clin Oncol* 2012;30:1553–61.
 36. Zwaveling J, Press RR, Bredius RG, van Derstraaten TR, den Hartigh J, Bartelink IH, et al. Glutathione S-transferase polymorphisms are not associated with population pharmacokinetic parameters of busulfan in pediatric patients. *Ther Drug Monit* 2008;30:504–10.
 37. Yeh RF, Pawlikowski MA, Blough DK, McDonald GB, O'Donnell PV, Rezvani A, et al. Accurate targeting of daily intravenous busulfan with 8-hour blood sampling in hospitalized adult hematopoietic cell transplant recipients. *Biol Blood Marrow Transplant* 2012;18:265–72.
 38. Bartelink IH, van Kesteren C, Boelens JJ, Egberts TC, Bierings MB, Cuvelier GD, et al. Predictive performance of a busulfan pharmacokinetic model in children and young adults. *Ther Drug Monit* 2012;34:574–83.
 39. Nguyen L, Paci A, Vassal G. Population pharmacokinetics of busulfan in children—letter. *Clin Cancer Res* 2012;18:2715–6; author reply 2157–8.
 40. Schechter T, Finkelstein Y, Doyle J, Verjee Z, Moretti M, Koren G, et al. Pharmacokinetic disposition and clinical outcomes in infants and children receiving intravenous busulfan for allogeneic hematopoietic stem cell transplantation. *Biol Blood Marrow Transplant* 2007;13:307–14.
 41. Vassal G, Michel G, Esperou H, Gentet JC, Valteau-Couanet D, Doz F, et al. Prospective validation of a novel IV busulfan fixed dosing for paediatric patients to improve therapeutic AUC targeting without drug monitoring. *Cancer Chemother Pharmacol* 2008;61:113–23.
 42. Veal GJ, Nguyen L, Paci A, Riggi M, Amiel M, Valteau-Couanet D, et al. Busulfan pharmacokinetics following intravenous and oral dosing regimens in children receiving high-dose myeloablative chemotherapy for high-risk neuroblastoma as part of the HR-NBL-1/SIOPEN trial. *Eur J Cancer* 2012;48:3063–72.
 43. Holford NH, Buclin T. Safe and effective variability—a criterion for dose individualization. *Ther Drug Monit* 2012;34:565–8.
 44. Holford NH, Ma SC, Anderson BJ. Prediction of morphine dose in humans. *Paediatr Anaesth* 2012;22:209–22.